IOPscience iopscience.iop.org

Home Search Collections Journals About Contact us My IOPscience

A first principles investigation of stacking fault energies and bonding in wurtzite materials

This article has been downloaded from IOPscience. Please scroll down to see the full text article.

1999 J. Phys.: Condens. Matter 11 5057

(http://iopscience.iop.org/0953-8984/11/26/308)

View the table of contents for this issue, or go to the journal homepage for more

Download details:
IP Address: 171.66.16.214
The article was downloaded on 15/05/2010 at 12:00

Please note that terms and conditions apply.

J. Phys.: Condens. Matter **11** (1999) 5057–5063. Printed in the UK PII: S0953-8984(99)04029-1

A first principles investigation of stacking fault energies and bonding in wurtzite materials

J A Chisholm and P D Bristowe

Department of Materials Science and Metallurgy, University of Cambridge, Pembroke Street, Cambridge CB2 3QZ, UK

E-mail: jac54@cus.cam.ac.uk and pdb1000@cus.cam.ac.uk

Received 6 May 1999

Abstract. Basal plane stacking fault energies for GaN, AlN, InN and BeO are calculated using density functional theory. A relation which links the stacking fault energy to a parameter of the material is sought in order to explain the different stacking fault concentrations observed in each material. An investigation into fully relaxed structures shows that the formation energy is lower in materials with higher *c/a* ratios. A Mulliken population analysis shows that for the case of the group-III nitrides the stacking fault energy increases monotonically with increasing Mulliken charge.

1. Introduction

GaN, AlN, InN and their related alloys are important materials for the fabrication of electronic devices, such as blue light emitting diodes, laser diodes and high temperature, high pressure transistors [1]. Of particular value is the ability to tailor the band gap from 1.9 eV (InN) to 6.2 eV (AlN) by changing the alloy composition. BeO is an insulating ceramic which, due to its high dielectric strength, can be used in high frequency circuits. The importance of defects is well recognized and much work has been carried out, especially in GaN, to determine what effect defects, such as inversion domain boundaries, dislocations and stacking faults, have on the electrical and optical properties of the material. Recently the energetics and electronic structure of stacking faults in AlN, GaN and InN were investigated by Stampfl and Van de Walle [2]. Their findings show that the formation energies increased in the order GaN, InN and AlN for three types of stacking fault and that no electronic levels are introduced into the band gap. These fault energies agree with measurements by Suzuki *et al* [3] on the width of 60° dislocations using high resolution transmission electron microscopy (HRTEM). In this investigation a good correlation was found between the reduced stacking fault energy (SFE) of ‘type two’ stacking faults in ZnO, BeO, AlN, GaN and InN and the *c/a* ratio for the unit cell, in which the SFE reduced almost exponentially with increasing *c/a*. Previous investigations have found correlations between the SFE and Phillip’s ionicity f_i [4] and the charge redistribution index s [5], both of which are physical parameters indicating the nature of the bonds. As yet such relations have not been investigated from a purely theoretical approach. The aim of this investigation is to calculate stacking fault energies and bonding characteristics in AlN, InN, GaN and BeO from first principles and so to explore the reasons for the range in stacking fault energies in these materials.

0953-8984/99/265057+07$19.50 © 1999 IOP Publishing Ltd

2. Computational method

Calculations are based on density functional theory (DFT) in the local density approximation (LDA) and employ Kerker norm conserving non-local pseudopotentials. Electron wavefunctions are expanded in terms of a plane wave basis set and the electronic ground state is reached using a conjugate gradients minimization scheme, as implemented by the computer code CETEP. The methodology employed by this code is described in a review by Payne *et al* [6] and is considered the most appropriate for the present application, because of its ability to determine defect energies and lattice parameters to high accuracy. In order to investigate bonding characteristics, a Mulliken population analysis is carried out on the self-consistent eigenstates. This analysis gives two quantities which give an insight into the strength of bonding and the gross charges on atoms: the overlap population and the Mulliken charge.

In order to relate to experimental values, calculations are carried out on 'type two' stacking faults in which the stacking sequence of the perfect cell in the [0001] direction, $a\alpha b\beta a\alpha b\beta a\alpha b\beta$, is changed to $a\alpha b\beta c\gamma b\beta c\gamma b\beta$. This fault is illustrated in figure 1 which shows a region of sphalerite extending for eight (0001) layers. Stacking fault energies can thus be expected to mirror wurtzite–sphalerite energy differences. To compute the stacking

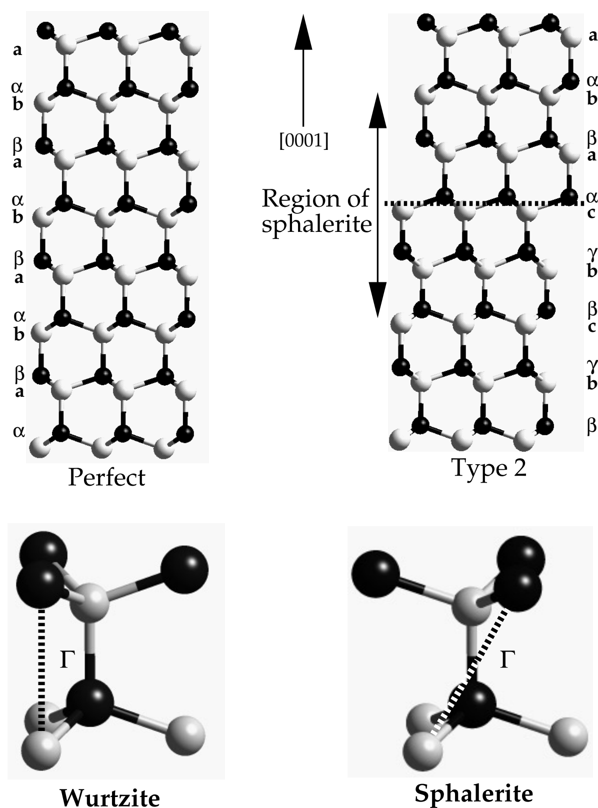

Figure 1. The [0001] stacking sequence in the perfect wurtzite structure is compared to the stacking sequence of a type 2 stacking fault. The fault introduces a region of sphalerite which results in an increase in the third nearest neighbour distance Γ.

fault energies, the ground state energy of a 20 atom unfaulted cell is compared to that of a 20 atom cell containing two evenly spaced 'type two' stacking faults. Atomic coordinates and cell dimensions are allowed to relax fully in all cases according to the Brodgen–Fletcher–Goldfarb–Shanno Hessian update scheme. The energy differences are small, being of the order of tens of meV, and therefore accurate calculations are required. The cutoff energy for the plane wave basis set is chosen to be 780 eV for AlN, 800 eV for InN, 800 eV for GaN and 900 eV for BeO. Tests show that these values ensure energy differences between faulted and unfaulted cells are converged to meV accuracy. The different values reflect the relative hardnesses of the pseudopotentials. Eight k-points are employed for each cell in the investigation and are chosen according to the commonly used Monkhorst–Pack scheme [7]. This corresponds to a k-point spacing of 0.10 $Å^{-1}$ and again ensures meV accuracy in the faulted–unfaulted cell energy differences. The d electrons are included as valence electrons for InN and GaN in order to reproduce the correct lattice parameters and accurate *c/a* ratios.

3. Results and discussion

The results of this investigation are plotted in figure 2(a) which shows the variation of fault energy with the fully relaxed *c/a* ratio. There is a good correlation with SFE which is found to be lower in those wurtzite materials with higher *c/a* ratios. It can also be seen from this figure that the SFE is extremely sensitive to this ratio. The trend is similar to that found by Suzuki *et al* [3] except that the actual magnitudes do vary. For example, stacking fault energies are lower by 30% for the case of AlN and higher by 50% for the case of InN. On the other hand, all *c/a* ratios are within 0.6% of experimental values. These values are shown in table 1, which also shows reasonable agreement with Stampfl and Van de Walle's calculations [2] on 'type two' faults and Wright's determination of fault energies using the Ising model [8]. Two points of interest, however, are the lower value for AlN and the slightly higher value for InN. Table 1 also shows the wurtzite–sphalerite structural energy differences for each material. These energies are higher than the SFE, as expected, and the trend with the *c/a* ratio is repeated.

Table 1. Calculated stacking fault energies and *c/a* ratios. Values are compared to experimental measurements and other DFT calculations: [a] this paper; [b] [3]; [c] [8]; [d] [2].

Material	AlN	InN	GaN	BeO
Stacking fault energy[a] (meV)	77	58	20	25
c/a ratio of relaxed cell [a]	1.609	1.613	1.630	1.625
HRTEM measurements[b] (meV)	115 ± 36	27 ± 6		16 ± 3
Experimental *c/a* ratio [b]	1.600	1.611		1.623
Other DFT calculations[c] (meV)	103	44	24	
Other DFT calculations[d] (meV)	109	52	22	
wz–sp energy difference[a] (meV)	104	72	25	27

The question remains as to why there should be a relationship between the stacking fault energy and the *c/a* ratio. The difference between the faulted and unfaulted structures is quite subtle. One way in which this can be viewed is by considering the distance between third nearest neighbour atoms, Γ, as shown in figure 1. This distance increases in transforming from the wurtzite to the sphalerite phase which, for the case of wurtzite materials, is accompanied by an increase in the total energy. It may therefore be expected that the SFE should be dependent on the increase in Γ. In order to investigate this, the change in Γ is obtained from measurements on the relaxed faulted and unfaulted cells.

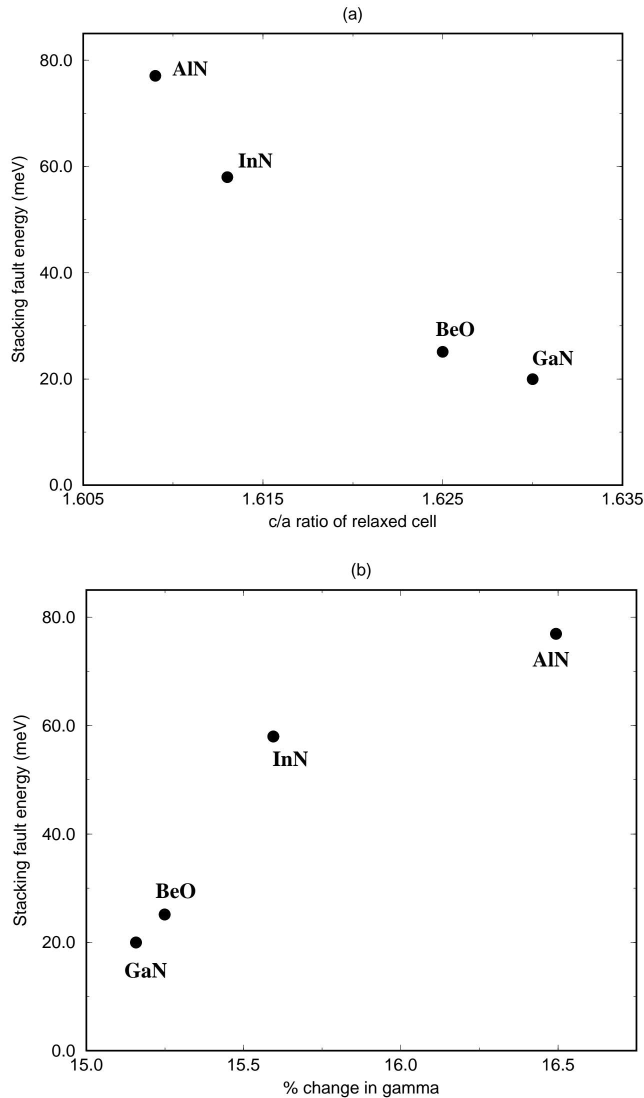

Figure 2. (a) The computed SFE as a function of *c/a* ratio. The monotonic trend is similar to experimental results [3]. (b) The computed SFE as a function of percentage change in Γ, the third nearest neighbour distance. The figure demonstrates that the SFE depends on changes in interatomic distances in transforming from the unfaulted to the faulted structure.

The results are plotted in figure 2(b), which shows that the SFE increases monotonically with increasing percentage change in Γ. This demonstrates that the SFE depends on changes in interatomic distances in transforming from the unfaulted to the faulted structure. This percentage change in Γ is determined solely by the *c/a* ratio with smaller *c/a* ratios leading to higher percentage changes in Γ and vice versa. Hence stacking fault energies are lower in materials with higher *c/a* ratios.

The DFT calculations contain accurate information on the distribution of charge in the supercells and it is of interest to use this information to find the relative Mulliken charges and bond strengths of the four materials and to investigate any relation with stacking fault

energy. In order to investigate bonding characteristics a population analysis is carried out on the electronic wavefunctions. This analysis follows that of Mulliken [9] in which the electron population is divided up into overlap and 'atomic' regions to give two quantities: the Mulliken charge on an atom A and the overlap population between two atoms A and B. The Mulliken charge is defined as

$$Q_M(A) = \sum_k w_k \sum_{\mu}^{on\,A} \sum_{\nu} P_{\mu\nu}(k) S_{\mu\nu}(k) \tag{1}$$

and the overlap population as

$$n_M(AB) = \sum_k w_k \sum_{\mu}^{on\,A} \sum_{\nu}^{on\,B} 2P_{\mu\nu}(k) S_{\nu\mu}(k) \tag{2}$$

where w_k are the weights of the k-points in the original total energy calculation, $P_{\mu\nu}(k)$ is the density matrix containing information on the distribution of charge and $S_{\mu\nu}(k)$ is the overlap matrix which measures the degree of overlap of the basis set. The concepts of 'atomic' and overlap populations were developed in terms of a linear combination of atomic orbitals (LCAO) basis set. Therefore, to carry out the analysis, the electron wavefunctions were projected from a plane wave to an atomic orbital basis set according to the projection scheme of Sanchez-Portal *et al* [10]. The atomic orbitals used were the pseudoatomic orbitals employed in the construction of the relevant pseudopotential. Both the projection scheme and the population analysis are implemented by the overlap code of Segall *et al* [11] which has been shown to give useful information on the nature of bonds in bulk materials.

The results of the analysis are presented in table 2 which shows overlap populations for nearest neighbours in both the wurtzite and the sphalerite phase. The overlap population can be positive, indicating a bonding state, or negative, indicating an anti-bonding state, with increasing overlap populations representing increasing strengths of covalent bonding.

Table 2. Overlap populations for nearest neighbours and Mulliken charges on the cation of the species in the wurtzite and sphalerite phases. It is noted that the wurtzite phase has two bond lengths and therefore two values for the overlap population. K is the experimental bulk modulus. Also shown is the change in Coulomb energy ΔE_C between third nearest neighbours as calculated from the expression for electrostatic potential energy. References: [a] [12]; [b] [13]; [c] [14]; [d] [15].

Material	Overlap n_M (wz)	n_M (sp)	K (GPa)	Q_M ($\|e\|$) (wz)	Q_M ($\|e\|$) (sp)	ΔE_C (meV)
AlN	0.514, 0.543	0.545	210[a]	1.327	1.300	123
InN	0.440, 0.462	0.466	139[b]	1.215	1.201	94
GaN	0.549, 0.589	0.589	245[c]	0.987	0.969	76
BeO	0.458, 0.510	0.511	211[d]	0.768	0.754	78

It can be seen that GaN has the strongest bonding and that InN is predicted to have the weakest. This result is found to be in good agreement with experimental values of bulk modulus [12–15]. There is no obvious correlation between the overlap population and the SFE which indicates that the SFE depends little on strength of bond. It is interesting to note that the overlap population for nearest neighbours are higher in the sphalerite phase, indicating relatively higher bond strengths for sphalerite. However, there is no obvious relation between the SFE and the change in overlap population which indicates that any change in bond energy contributes little to the stacking fault energy.

Table 2 also shows the Mulliken charge (Q_M) for all materials in both the wurtzite and the sphalerite phase. This quantity gives a measure of the amount of charge transferred between anions and cations. Thus, for example, a Mulliken charge of 0.987 on a Ga ion means that

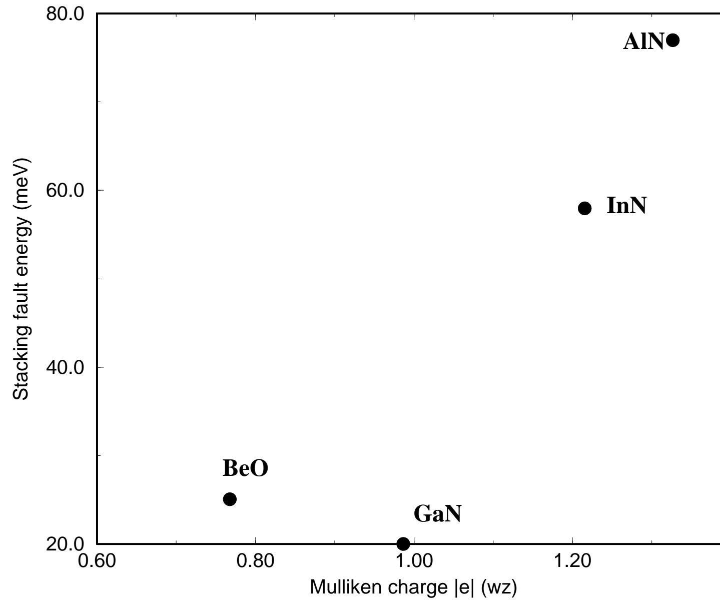

Figure 3. The computed SFE as a function of Mulliken charge. For the case of the group-III nitrides the SFE increases monotonically with increasing Mulliken charge.

0.987 electrons have transferred to the N anion. These charges are sensitive to the atomic basis set and therefore, in general, absolute values of Q_M should be handled with care. However, tests show that the relative order of the Mulliken charges, i.e., BeO having the lowest and AlN having the highest value, is unaffected by the use of alternative basis sets.

For the group-III nitrides the SFE increases monotonically with increasing Mulliken charge as shown in figure 3. This can be readily understood by considering the increases in Coulomb energy as third nearest neighbour anions and cations are moved further apart in transforming from the unfaulted to the faulted structure. This increase in Coulomb energy is naturally greater for larger Mulliken charges. However, the trend does not obviously apply to BeO and it is clear that the SFE is not determined by Q_M alone. The Mulliken charges together with the fully relaxed structures allows the relative changes in Coulomb energy between the unfaulted and faulted structures to be calculated using a simple expression for the electrostatic potential energy. Values for the change in Coulomb energy obtained by such a simplistic calculation are shown in table 2. The change in Coulomb energy between the faulted and unfaulted structures follows the trend for the stacking fault energies which suggests that the two are directly related. BeO does not follow the trend of SFE versus Mulliken charge because changes in interatomic distances are more pronounced and the dielectric constant is significantly lower in BeO than in the group-III nitrides.

4. Conclusions

In summary, we have calculated the stacking fault energies, overlap populations and Mulliken charges for AlN, InN, GaN and BeO using density functional theory. A clear relation was found between the SFE and the *c/a* ratio of the unit cell in which the SFE decreased monotonically with increasing *c/a* in agreement with experimental observations [3]. This was explained

by showing how the change in third nearest neighbour distance Γ, and hence the change in Coulomb energy, is more pronounced in those materials with higher *c/a* ratios. A Mulliken population analysis has shown that the bonds are weaker and the Mulliken charges greater in the wurtzite phase for all materials. We conclude that both the strength of covalent bond and the change in bond energy contribute little to the stacking fault energy and that, for the group-III nitrides, the SFE is determined by the Mulliken charge.

Acknowledgments

The authors acknowledge the support of EPSRC grants in providing time on the Cray T3E parallel machine at the Edinburgh Parallel Computing Centre, UK. Thanks are also due to M Segall, P Hasnip, M Jarvis and C Pickard for useful discussions.

References

[1] Morkoç H 1997 *Materials Science Forum* **239–241** 119
[2] Stampfl C and Van de Walle C G 1998 *Phys. Rev.* B **57** R15 052
[3] Suzuki K, Ichihara M and Takeuchi S 1994 *Japan. J. Appl. Phys.* **33** 1114
[4] Gottschalk H, Patzer G and Alexander H 1978 *Phys. Status Solidi* a **45** 207
[5] Takeuchi S, Suzuki K, Maeda K and Iwanaga H 1984 *Phil. Mag.* A **50** 171
[6] Payne M C, Teter M P, Allan D C, Arias T A and Joannopoulos J D 1992 *Rev. Mod. Phys.* **64** 1045
[7] Monkhorst H J and Pack J D 1976 *Phys. Rev.* B **13** 5188
[8] Wright A F 1997 *J. Appl. Phys.* **82** 5259
[9] Mulliken R S 1955 *J. Chem. Phys.* **23** 1833
[10] Sanchez-Portal D, Artacho E and Soler J M 1995 *Solid State Commun.* **95** 685
[11] Segall M D, Shah R, Pickard C J and Payne M C 1996 *Phys. Rev.* B **54** 16 317
[12] McNeil L E, Grimsditcha M and French R H 1993 *J. Am. Ceram. Soc.* **76** 1132
[13] Sheleg A U and Savastenko V A 1979 *Izv. Akad. Nauk SSSR, Neorg. Mater.* **15** 1598
[14] Perlin P, Jauberthie-Carillon C, Itie J P, San Miguel A, Grzegory I and Polian A 1992 *Phys. Rev.* B **45** 83
[15] Alper A M (ed) 1970 *High Temperature Oxides* part III (New York: Academic)